

Oxygen Vacancy-Dependent Low-Temperature Performance of Ni/CeO₂ in CO₂ Methanation

Luliang Liao^{b,†}, Kunlei Wang^{a,†}, Guangfu Liao^{c*}, Muhammad Asif Nawaz^{d*}, Kun Liu^{a*}

^a School of Resources and Environment, Nanchang University, 999 Xuefu Road, Nanchang, Jiangxi, 330031, China

^b Jiangxi Science Technology Normal University, Nanchang, Jiangxi, China

^c College of Materials Engineering, Fujian Agriculture and Forestry University, Fuzhou 350002, China

^d Department of Inorganic Chemistry and Material Sciences Institute of Seville (ICMSE), University of Seville-CSIC, Seville 41092, Spain

* Corresponding author. E-mail: liaogf@mail2.sysu.edu.cn (G. Liao), mnawaz@us.es (M. A. Nawaz), liukun@ncu.edu.cn (K. Liu)

† These authors contributed equally

Content

S1 Characterization	2
S2. Supplementary Figure	3
S3. Supplementary Table	5
S4. References	7

S1 Characterization

The performance of the catalyst is significantly influenced by its pore structure. X-ray diffraction (XRD) was employed with Cu K α radiation ($\lambda = 1.5405 \text{ \AA}$), scanning 2θ angles from 10 to 90° at a speed of $2^\circ/\text{min}$, using a 30 mA tube current and 40 kV tube voltage. Micromeritics ASAP-2020 surface area analyzer was utilized for catalyst surface area analysis. Prior to testing, catalyst samples were vacuum-degassed at 250°C for 3 hours, followed by N_2 adsorption-desorption at -196°C to obtain BET surface area and pore volume, with pore size distribution determined using the BJH method. Raman analysis, conducted on a Renishaw spectrometer with a laser wavelength of 532 nm , explored surface defects over a range of 200 to 900 cm^{-1} . CO_2 -TPD, crucial for investigating catalyst surface basicity, was performed using a Micromeritics AutoChem 2920 chemisorption analyzer. XPS, based on the photoelectric effect, facilitated qualitative and semi-quantitative/quantitative elemental and chemical state analysis of solid surfaces, utilizing a PHI 5000 CESCAs System with Al/Mg anode, operating at 14.0 kV and 250 W , with vacuum conditions better than $1 \times 10^{-8} \text{ Torr}$. Binding energy was calibrated with $\text{C } 1s = 284.6 \text{ eV}$ as the reference. In-situ FTIR, crucial for

capturing intermediate species and elucidating reaction mechanisms, employed a Bruker instrument featuring a highly sensitive MCT detector. Prior to experimentation, samples underwent pretreatment at 300 °C in high-purity Ar, followed by cooling to 50 °C and background correction under Ar. Subsequently, a mixed gas (4% H₂, 1% CO₂, 95% Ar) was introduced for CO₂ hydrogenation testing, with a gas flow rate of 20 mL/min, ramping from 50 °C to 400 °C to monitor dynamic changes in intermediate species until reaching a steady state.

S2. Supplementary Figure

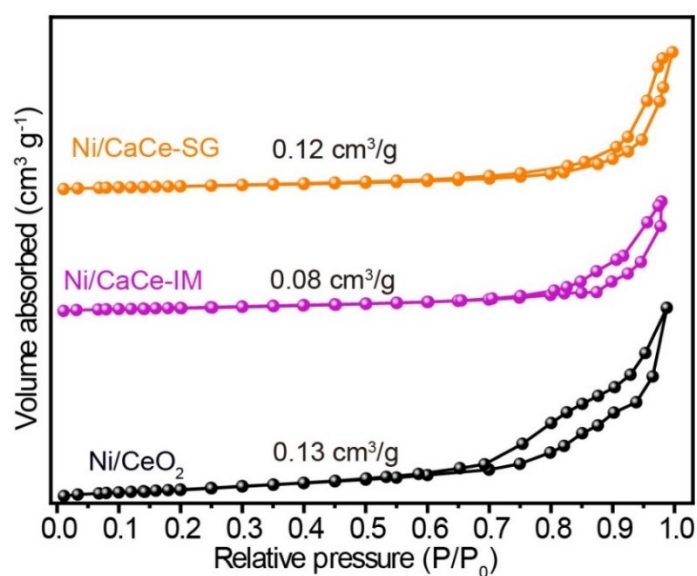


Figure S1. N₂ adsorption and desorption of the Ni/CaCe catalysts.

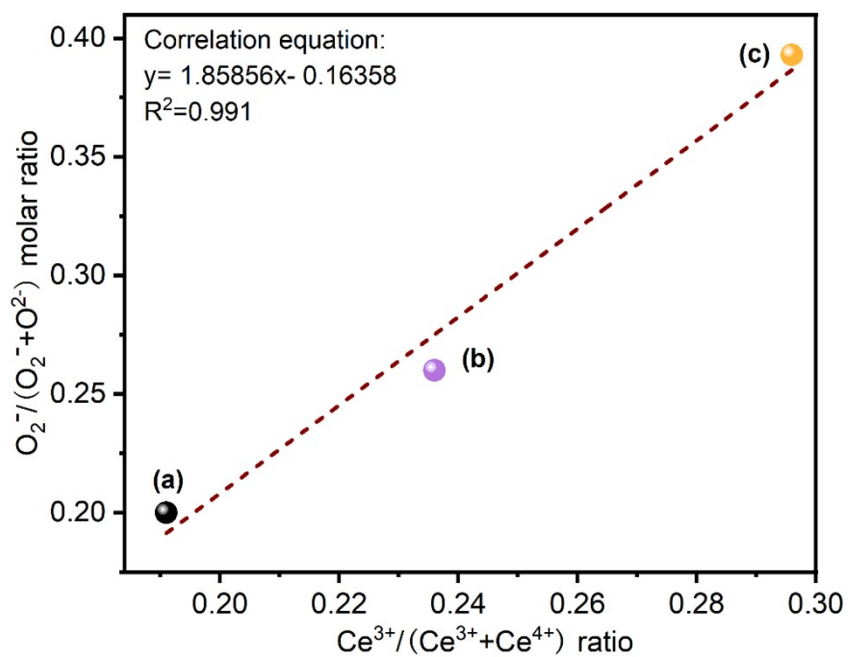


Figure S2. Surface $\text{O}_2\cdot^-/(\text{O}_2\cdot^- + \text{O}_2^{2-})$ molar ratios versus $\text{Ce}^{3+}/(\text{Ce}^{3+} + \text{Ce}^{4+})$ ratios on the Ni/CaCe catalysts. (a) Ni/CeO₂, (b) Ni/CaCe-IM, (c) Ni/CaCe-SG.

S3. Supplementary Table

Table S1 Quantitative results of O₂⁻ surface oxygen vacancies.

Supports	I ₅₇₀ /I ₄₆₀ (×10 ⁻²)	I ₁₀₆₈ /I ₄₆₀ (×10 ⁻²)
CeO ₂	0.8	1.2
CaCe-IM	1.2	1.5
CaCe-SG	4.6	4.4

Table S2 Quantitative results of XPS

Catalysts	Relative amount (%)			O ₂ ⁻ / (O ₂ ⁻ +O ²⁻) ^a (%)	Ce ³⁺ / (Ce ³⁺ +Ce ⁴⁺) ^a (%)	M/ (Ce+M) molar ratio ^b
	O ₂ ^{- a}	CO ₃ ^{2- a}	O ^{2- a}			
Ni/CeO ₂	17.5	14.4	68.1	20.3	19.1	-
Ni/CaCe-IM	16.3	35.3	48.4	26.0	23.6	0.096
Ni/CaCe-SG	28.1	24.6	47.3	39.3	29.6	0.091

^a Measured by XPS.

^b Measured by ICP.

Table S3 Quantitative results of the activation energy and reaction rate

Catalysts	R _w ^a (250 °C) [10 ⁻³ mmol s ⁻¹ g ⁻¹]	R _S ^b (250 °C) [10 ⁻⁴ mmol s ⁻¹ m ⁻²]	E _a ^c [kJ mol ⁻¹]
Ni/CeO ₂	3.0	1.4	111
Ni/CaCe-IM	6.6	3.9	104
Ni/CaCe-SG	11.6	6.9	82

Table S4 Quantitative results of H₂-TPD

Catalysts	Ni contents (wt%) ^a	H ₂ desorption amount (μmol g ⁻¹)	Metallic Ni surface area (m ² g _{Ni} ⁻¹) ^b	Dispersion (%) ^b	TOF _{CO2} (s ⁻¹) ^c
Ni/CeO ₂	9.3	38.8	20.8	2.5	0.03
Ni/CaCe-IM	9.2	50.8	26.5	3.1	0.07
Ni/CaCe-SG	9.2	60.9	31.8	3.9	0.10

^aDetermined by ICP.

^bPt/Al₂O₃ (D = 34.5%) was used as the standard. Based on the cross-sectional area of one surface Ni atom, 8.24×10^{-20} m².

^cCalculated based on the steady state CO₂ conversion at 250 °C.

Table S5 Quantitative results of CO₂-TPD

Catalysts	Weak alkaline site amount (μmol m ⁻²)	Moderate alkaline site amount (μmol m ⁻²)	Total amount below 450 °C (μmol m ⁻²)
Ni/CeO ₂	1.2	1.1	2.3
Ni/CaCe-IM	1.3	1.9	3.1
Ni/CaCe-SG	1.9	2.5	4.5

Table S6 A literature summary of Ni-based catalysts in CO₂ methanation

Entry	Catalysts	Ni% (wt%)	Reaction condition			GHSV (mL/g _{cat} h)	CO ₂ conver sion (%)	Ref
			S _{BET} (m ² /g)	T (°C)	P (bar)			
1	2Ni-2Co /CeO ₂	2	-	290	1	12000	5	[1]
2	2Ni-2Mn/CeO ₂	2	-	290	1	12000	4	[1]
3	Ni/CeO ₂ -10	10	27.9	275	1	30000	28	[2]
4	NiCe/ZrO ₂	10	5.2	350	1	18000	48	[3]
5	NiLa/ZrO ₂	10	6	350	1	18000	37	[3]
6	Ni/CeO ₂	10	84	350	1	18000	55	[3]
10	NiO/CeO ₂	10	-	300	1	36000	58	[4]
11	Ni/CeO ₂ -NR	8	72	300	1	16500	68	[5]
12	10NiCe	10	-	300	1	72000	71	[6]
13	Ni/CeO ₂	2	31	275	1	30000	32	[7]
14	Ni/CeO ₂ -NR	8	72	275	1	30000	79	[8]
15	Ni/CaCe-SG	10	26	290	1	18000	77	This wok

S4. References

1. C. G. Wasnik, M. Nakamura, T. Shimada, H. Machida, K. Norinaga, *Carbon Resources Conversion*, 2024, 100241.
2. L. Li, L. Jiang, D. Li, J. Yuan, G. Bao, K. Li, *Appl. Catal. O: Open*, 2024, **192**, 206956.
3. R. A. El-Salamony, K. Acharya, A. S. Al-Fatesh, A. I. Osman, S. B. Alreshaidan, N. S. Kumar, H. Ahmed, R. Kumar, *Mol. Catal.*, 2023, **547**, 113378.
4. I. Martínez-López, J. C. Martínez-Fuentes, J. Bueno-Ferrer, A. Davó-Quñonero, E. Guillén-Bas, E. Bailón-García, D. Lozano-Castelló, A. Bueno-López, *J. CO₂ Util.*, **81**, 102733.

5. G. Varvoutis, A. Lampropoulos, P. Oikonomou, C.-D. Andreouli, V. Stathopoulos, M. Lykaki, G. E. Marnellos, M. Konsolakis, *J. CO₂ Util.*, 2023, **70**, 102425.
6. L. Atzori, M. G. Cutrufello, D. Meloni, F. Secci, C. Cannas, E. Rombi, *Int. J. Hydrogen Energy*, 2023, **48**, 25031-25043.
7. N. García-Moncada, J. C. Navarro, J. A. Odriozola, L. Lefferts, J. A. Faria, *Catal. Today*, 2022, **383**, 205-215.
8. G. Varvoutis, M. Lykaki, S. Stefa, E. Papista, S. A. C. Carabineiro, G. E. Marnellos, M. Konsolakis, *Catal. Commun.*, 2020, **142**, 106036.